

# Slow-spreading submarine ridges in the South Atlantic as a significant oceanic iron source

Mak A. Saito<sup>1\*</sup>, Abigail E. Noble<sup>1,2</sup>, Alessandro Tagliabue<sup>3,4</sup>, Tyler J. Goepfert<sup>1,2</sup>, Carl H. Lamborg<sup>3,1</sup> and William J. Jenkins<sup>1\*</sup>

**Low levels of the micronutrient iron limit primary production and nitrogen fixation in large areas of the global ocean. The location and magnitude of oceanic iron sources remain uncertain, however, owing to a scarcity of data, particularly in the deep ocean<sup>1</sup>. Although deep-sea hydrothermal vents along fast-spreading ridges have been identified as important contributors to the oceanic iron inventory<sup>2</sup>, slow-spreading ridges, which contribute more than half of the submarine ridge-crest environment, are assumed to be less significant and remain relatively unexplored<sup>2</sup>. Here, we present measurements of dissolved iron and manganese concentrations along a full-depth section in the South Atlantic Ocean, running from offshore of Brazil to Namibia. We detect a large dissolved iron- and manganese-rich plume over the slow-spreading southern Mid-Atlantic Ridge. Using previously collected measurements of helium-3 concentrations—a tracer of hydrothermal activity—we calculate the ratio of dissolved iron to hydrothermal helium in the plume waters and find that it is 80-fold higher than that reported for plume waters emanating from faster-spreading ridges in the southeastern Pacific<sup>3</sup>. Only the application of a higher ratio in global ocean model simulations yields iron fluxes from these slow-spreading submarine ridges that are in line with our observations. We suggest that global iron contributions from hydrothermal vents are significantly higher than previously thought, owing to a greater contribution from slow-spreading regions.**

Since their discovery in the late 1970s, hydrothermal vents have captivated marine geochemists and biologists with their billowing high-temperature seawater plumes enriched with chemical elements<sup>4</sup> and the unique deep-ocean ecosystems that surround them. The elemental fluxes from hydrothermal vents and their relationship to source rocks have been studied<sup>5,6</sup>, yet estimating the contribution of hydrothermal vents to whole-ocean inventories for elements with complex chemistries such as iron has been particularly challenging<sup>7,8</sup>. This difficulty stems from the rapid removal of metals from the high-temperature buoyant plumes during mixing with surrounding waters and the transformation into neutrally buoyant plumes. During mixing most of the iron is precipitated to sediments as iron sulphides in close proximity to the vent fields, or as iron oxides on further interaction with surrounding oxygenated sea water<sup>7,9</sup>. As a result the contribution of hydrothermal vents to the overall dissolved oceanic inventories of iron and other metals has been difficult to constrain because only a small fraction survives precipitation and loss to sediments<sup>7,9</sup>.

A recent modelling study estimated the global hydrothermal iron flux by using global mantle helium-3 (<sup>3</sup>He) fluxes along all ocean ridge systems and calculating an iron flux using a representative dissolved iron–helium ratio<sup>2</sup> (dFe:<sup>3</sup>He). These iron fluxes were introduced into a state-of-the-art global ocean circulation and biogeochemistry model complete with iron equilibrium and scavenging chemical parameterizations, resulting in an upward revision of the estimated hydrothermal vent contribution to the whole ocean inventory by threefold over previous estimates to  $9 \times 10^8$  mol dFe yr<sup>-1</sup>. This model study<sup>2</sup> assumed a uniform dFe:<sup>3</sup>He ratio taken from water column values downstream of the southern Pacific Ridge<sup>3</sup> at 20° S 170° W thereby incorporating some of the chemical complexity of localized vent precipitation. As a result, spatial variability in the hydrothermal Fe flux was implicitly driven by ridge spreading rates with the fast-spreading ridges in the Pacific Ocean estimated to be significant iron sources, whereas the slow-spreading Mid-Atlantic Ridge (MAR) introduced little hydrothermal Fe. There is substantial variability documented<sup>2</sup> in near-field measures of the dFe:<sup>3</sup>He ratio, which implies that there is potential for hydrothermal sources of Fe and <sup>3</sup>He to be decoupled. If this were true, then it could be that ridge spreading rate is not the first-order control on the hydrothermal Fe flux, and that regions of slow rates of seafloor spreading, such as the MAR, could be a more important source of Fe than of <sup>3</sup>He. As such regions account for more than half of the submarine ridge-crest environment and are relatively unexplored, it would imply that these recent estimates of hydrothermal Fe input remain significant underestimations.

Here we present a large water column iron and manganese data set that demonstrates that the slow-spreading ridge system of the Southern Atlantic contributes a significant hydrothermal iron flux to the South Atlantic Basin. On the 2007 CoFeMUG expedition (Co, Fe and microbes from the upwelling to the gyre) from Brazil to Namibia in the South Atlantic Ocean, we sampled a full-depth ocean section (Fig. 1 and Supplementary Table S1), to create the first basin-scale full-depth chemical section of iron and manganese for this region. The resulting data set identified a large plume of dFe and dissolved Mn (dMn) over the MAR between 1,500 m and 3,500 m depth with a width in excess of 1,000 km (Fig. 2a,b; distance between stations 5 and 9 was 1,087 km). Near the plume centre (12.5° S 15° W), the maximum dFe and dMn concentrations we observed were 1.9 nM and 1.4 nM at 2,841 m and 2,500 m depth, respectively (Fig. 2). The concentrations and large geographic scale of this South Atlantic dFe and dMn plume are comparable to those recently observed over or in the vicinity

<sup>1</sup>Marine Chemistry and Geochemistry Department, Woods Hole Oceanographic Institution, Woods Hole, Massachusetts 02543, USA, <sup>2</sup>Massachusetts Institute of Technology—Woods Hole Oceanographic Joint Program in Chemical Oceanography, Woods Hole, Massachusetts 02543, USA, <sup>3</sup>Department of Earth, Ocean and Ecological Sciences, School of Environmental Sciences, University of Liverpool, 4 Brownlow Street, Liverpool L69 3GP, UK, <sup>4</sup>Southern Ocean Carbon and Climate Observatory, CSIR, Cape Town 7700, South Africa. \*e-mail: msaito@whoi.edu; wjenkins@whoi.edu

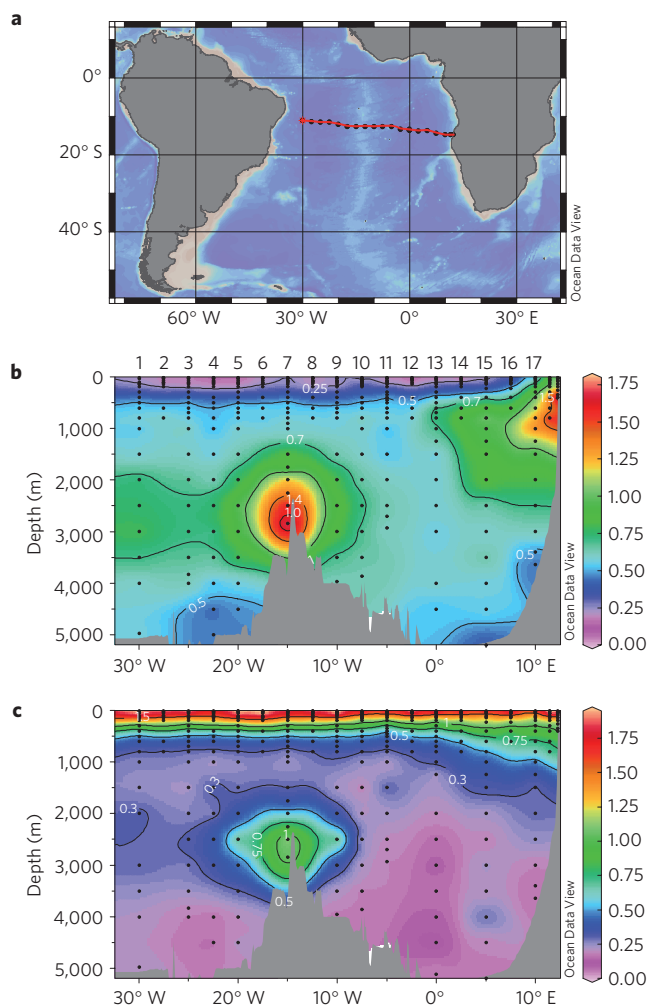


**Figure 1 | A zonal section of dFe and dMn in the South Atlantic.**

**a**, Sampling locations for seawater dFe and dMn during the RV *Knorr* CoFeMUG expedition in November–December 2007. **b,c**, Total dFe (**b**; nM) and dMn (**c**; nM) distributions reveal a large plume centred over the MAR at ~2,900 m depth and 2 km in height (station numbers shown over **b**).

of regions of fast-spreading ridges in the Pacific and Southern oceans<sup>10–12</sup>. Water column chemical speciation processes, such as complexation by organic ligands<sup>8,13</sup> and the formation of iron-sulphide colloidal nanoparticles<sup>14</sup>, are probably critical to protecting this iron from scavenging losses during long-range advection observed in this ocean section.

Regions of slow spreading rates and low <sup>3</sup>He fluxes have been considered to be indicative of lower hydrothermal activity<sup>2,5,15–17</sup>; however, recent discoveries of hydrothermal vent fields at slow and ultra-slow spreading ridges in the South Atlantic and elsewhere have led to a re-evaluation of the mechanisms for venting and the suggestion that hydrothermalism may occur along all mid-ocean ridge systems<sup>5,15</sup>. The iron plume described here also implies important hydrothermal iron sources in the South Atlantic, yet its specific source remains uncertain. Three vent fields have been previously described on the southern MAR (refs 15,18–20): the Turtle Pits hydrothermal field at 5° S, the Nibelungen field at 8° 18' S and the Lilliput field at 9° 33' S (Supplementary Fig. S1). Although Lilliput is the closest of the three to the observed plume at 12.5° S, it is too shallow at 1,500 m and is located within the ridge axis with restricted mixing<sup>20</sup>. The Nibelungen field to the north is a possible source<sup>19</sup>, with a high-temperature black smoker found at 2,915 m depth outside the ridge axis, consistent with plumes tending to

rise several hundred metres from their source. It is believed that this field is driven by tectonic and deep heat sources, rather than by the magmatic processes that are typical of the fast-spreading Pacific ridge systems<sup>15,19</sup>.

To compare these South Atlantic iron observations with recent estimates of global hydrothermal iron flux, we calculated a dFe:<sup>3</sup>He ratio for this section. The inert helium isotope <sup>3</sup>He serves as a tracer of hydrothermal activity, forming large plumes in the vicinity of hydrothermal regions and correlating with ridge spreading rate<sup>16,21,22</sup>. A previous World Ocean Circulation Experiment expedition<sup>21</sup> on a nearly identical South Atlantic zonal section along 11° S observed a large hydrothermal helium plume with a striking resemblance to the dFe and dMn reported here (Supplementary Fig. S3), implying a common hydrothermal source. Yet South Atlantic hydrothermal <sup>3</sup>He concentrations were more than an order of magnitude lower than those of the Pacific, with an helium isotope anomaly ( $\delta^3\text{He}$ ) of only 2–3% above background levels compared with 35% and higher in the Pacific Basin<sup>16,22</sup>. This large discrepancy between basins has been attributed to the much slower spreading rates and resultant lower hydrothermal <sup>3</sup>He flux of the South Atlantic<sup>15,21</sup>. Having computed and gridded the volcanic <sup>3</sup>He distribution for this section (see Methods), we interpolated the gridded field onto the depths of our Fe and Mn samples and show the relationship in Fig. 2c. A type-2 linear regression for samples between the depths of 1,700 and 3,500 m and longitudes 2° W and 28° W produced an estimated molar dFe:<sup>3</sup>He ratio in the plume of  $70 \pm 30 \times 10^6$  (mol:mol, Fig. 2c and Table 1). Some scatter was observed and is largely owing to the fact that the <sup>3</sup>He measurements were made on a different cruise and hence geographic correspondence is not precise. As expected, this relationship is driven primarily by the station closest to the MAR (Fig. 2c, blue symbols and Supplementary Table S2). Comparison with previous Pacific Ocean dFe:<sup>3</sup>He estimates<sup>3</sup> (red line shown in Fig. 2c,  $9 \times 10^5$  mol:mol) shows the South Atlantic dFe:<sup>3</sup>He ratio to be ~80-fold higher. This difference is significant because the Pacific value was applied in the recent global hydrothermal flux estimate (middle blue line, described as the Hydrofe\*1 model simulation)<sup>2</sup> as a means to convert global hydrothermal helium flux to dFe flux and performed well in reproducing data from the Southern Ocean.

Three factors are likely to influence the observed variation in oceanic water column dFe:<sup>3</sup>He ratios. First, dFe is prone to scavenging removal whereas helium is inert, resulting in gradual decreases in the ratio with distance from the hydrothermal source. Indeed the estimated dFe:<sup>3</sup>He ratio is almost twofold higher when the analysis is limited to Station 7 over the MAR compared with the basin-section value reported above (Supplementary Table S2 for ratios over a range of distances from the MAR). Scavenging losses of iron probably also influence the previously reported South Pacific ratio owing to its distance from hydrothermal sources. Yet the rate of iron scavenging is also slowed by complexation with organic complexes<sup>7,13</sup> and the high dFe concentrations within the Pacific (~0.9 nM; ref. 3) and Atlantic (1.9 nM; Fig. 2c) hydrothermal plumes are consistent with this. As a result, the potential maximum scavenging contribution to the dFe:<sup>3</sup>He ratio in the South Pacific is roughly a twofold decrease, based on the ~1–2 nM solubility of dFe in sea water and the concentrations observed<sup>23</sup>. Second, the large difference in ratios between the South Atlantic and South Pacific is influenced by the ~20-fold greater <sup>3</sup>He abundances found in the South Pacific, with maximum <sup>3</sup>He values of ~1 fM versus 0.045 fM for the South Atlantic in these iron comparison studies<sup>3,16,21</sup>. This large difference in <sup>3</sup>He is an important distinction between basins, whose cause is attributed to the slower spreading rates of the MAR. Third, geological variations in water–rock interactions also probably contribute to higher dFe:<sup>3</sup>He ratios in the South Atlantic<sup>15,19,24</sup>. For example, hydrothermal vents on the northern MAR have high iron fluxes owing to serpentinization reactions occurring between

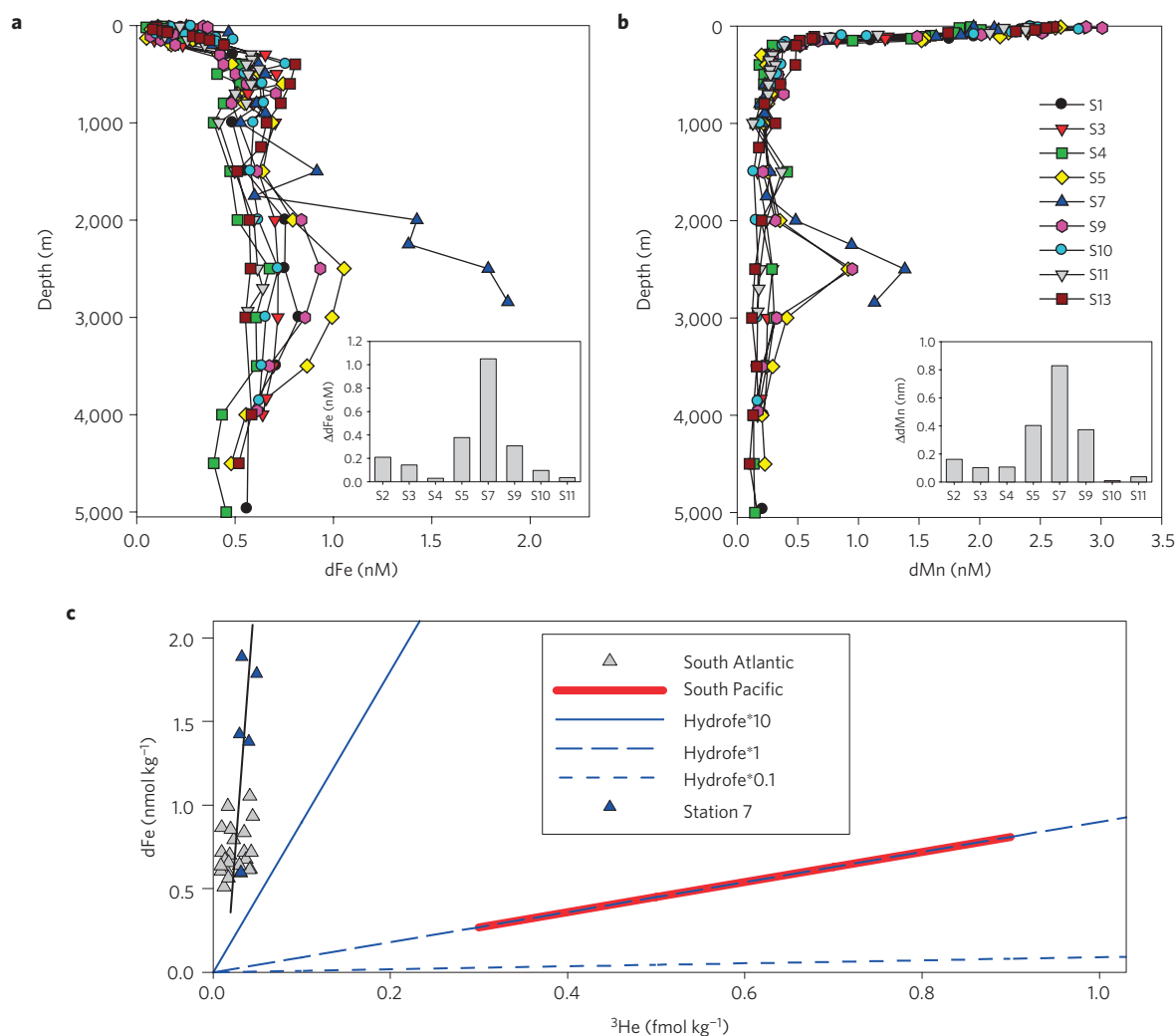


**Figure 2 | Vertical profiles from the vicinity of the MAR of the South Atlantic Ocean and comparison with <sup>3</sup>He distributions. a, b** dFe (a) and dMn (b) maxima over the centre of the MAR (station 7, bottom samples within 100 m of the bottom). Adjacent deep stations 5 and 9 showed a distinct influence of hydrothermal dFe and dMn, and were 1,087 km apart from each other. Insets:  $\Delta dFe$  and  $\Delta dMn$  represent the difference in average concentration between 2,000 m and 3,000 m depth for each station (S) and station 13, which was minimally affected by hydrothermal and coastal inputs.  $\Delta dFe$  and  $\Delta dMn$  show the hydrothermal plume contributions above background dFe and dMn levels and advection of the hydrothermal plume westwards also observed in the <sup>3</sup>He distribution<sup>21</sup> (Supplementary Fig. S3). **c**, Comparison of dFe measurements to volcanic <sup>3</sup>He distributions along 11° S. Previous <sup>3</sup>He data<sup>21</sup> were gridded and interpolated onto dFe from 1,700 m to 3,500 m depth between 2° W and 28° W and fit with a type-2 linear regression (black line, correlation present with 95% confidence; see Supplementary Table S2 for sensitivity analysis and statistics). As expected, the samples collected above the MAR showed the highest dFe and <sup>3</sup>He (in blue). The resulting dFe:<sup>3</sup>He ratio of  $70 \pm 30 \times 10^6$  was 80-fold higher than the South Pacific<sup>3</sup> (red line, covering the representative ranges of Pacific abyssal dFe and <sup>3</sup>He; refs 3,10,16). Although previous global model simulations<sup>2</sup> applied the South Pacific dFe:<sup>3</sup>He ratio parameter (Hydrofe\*1 simulation, middle blue dashed line), only a higher dFe:<sup>3</sup>He ratio (Hydrofe\*10, solid blue line) was able to reproduce the hydrothermal iron plume observed in the South Atlantic (unlike the Hydrofe\*1 and Hydrofe\*0.1 ratios) (Table 1 and Supplementary Fig. S4), but even this may be an underestimate for this location.

sea water and ultramafic rocks, a process that probably contributes to the water column iron plume observed here<sup>25</sup>.

This combination of the large hydrothermal dFe plume observed here and the estimated higher Atlantic dFe:<sup>3</sup>He ratio has important implications for improving global estimates of hydrothermal iron supply to the oceans. Comparison with output from the recent NEMO-PISCES 500-year global ocean hydrothermal model simulations<sup>2</sup> found that the dFe distributions observed in Fig. 1 were best reproduced by model runs with a tenfold higher dFe:<sup>3</sup>He ratio than used in the global hydrothermal model using the South Pacific value<sup>2</sup> (Table 1 and Supplementary Fig. S4). Moreover, pairing of abyssal dFe observations with model predictions ( $n = 87$ ) found a statistically significant correlation only for a dFe:<sup>3</sup>He ratio that was tenfold higher (the highest value

used,  $p$ -value =  $6.7 \times 10^{-8}$ ,  $R = 0.600$ , Table 1 and Supplementary Fig. S4), than that which achieved significant correlation for the Southern Ocean iron data set<sup>2</sup> (Table 1). Taken together, these comparisons demonstrate the better applicability of a higher dFe:<sup>3</sup>He ratio for the slow-spreading ridges to reproduce Fe fluxes, such as our observations in the South Atlantic Ocean. As slow-spreading ridges account for more than half of the total submarine global ridge crest<sup>5</sup>, this implies hydrothermal iron flux estimates could be a factor of two or more higher than previously estimated. More observations of Fe and <sup>3</sup>He near slow-spreading ridges are needed to better constrain the deep-ocean Fe cycle.

A future challenge for ocean chemistry research is bridging the gap between the discovery of individual hydrothermal vent fields and their role in basin-scale biogeochemical cycles. Coor-

**Table 1 | A statistical analysis between observations and modelled estimates of abyssal iron and calculated dFe:<sup>3</sup>He ratios.**

Experiment	Southern Ocean*		South Atlantic†			
	Mean dFe (nM)	R	Mean dFe (nM)	Slope	R	p-value
Data	0.563 (n = 104)		0.71 ± 0.26 (n = 87)			
Control	0.462	0.140	0.90 ± 0.16	0.190	0.094	0.444
Hydrofe*1	0.545	0.438	0.92 ± 0.15	0.437	0.197	0.105
Hydrofe*0.1	0.472	0.180	0.90 ± 0.16	0.226	0.110	0.368
Hydrofe*10	0.774	0.473	0.98 ± 0.13	1.47	0.600	6.727 × 10 <sup>-8</sup>
Ratio	Pacific water column‡		Atlantic water column§		Atlantic:Pacific	
dFe: <sup>3</sup> He (mol Fe/mol <sup>3</sup> He)	9.0 × 10 <sup>5</sup>		70 × 10 <sup>6</sup>		78	

\*Southern Ocean model data comparison (ref. 2) for 2–5 km depth<sup>30</sup>. †This study (CoFeMUG expedition) for 1.5–5 km depth. ‡From ref. 3. §This study, for 1.7–3.5 km depth, see Fig. 2c.

diation between the water column chemical mapping efforts of the GEOTRACES programme and future seafloor vent field exploration is critical for determining the location and extent of hydrothermal iron plumes. Our findings of a >1,000-km-wide plume of total dFe and dMn in the South Atlantic Basin imply that the slow-spreading ridges are more important iron sources than would be supposed from their spreading rates alone. Therefore, estimates of hydrothermal iron inputs that imply first-order control by ridge spreading rates are probably significant underestimates of this source's role in regulating the ocean's iron inventory.

## Methods

Samples were collected from the RV *Knorr* between 14 November 2007 and 13 December 2007 using trace metal clean 8 L X-Niskin sampling bottles deployed on an epoxy-coated rosette attached to a non-metallic line and were programmed to trip at predetermined depths. All sample bottles used to store sea water before analysis were soaked overnight in acidic detergent Citranox, rinsed thoroughly with Milli-Q water (Millipore), filled with 10% HCl to soak for ten days and rinsed thoroughly with Milli-Q water adjusted to pH 2. Immediately following collection during CoFeMUG, the X-Niskins were pressurized with 99.999% N<sub>2</sub> at ~5 psi and sea water was filtered through teflon tubing and a 144 mm, 0.4 µm polycarbonate plastic sandwich filter into acid-washed low-density polyethylene sample bottles in a positive pressure class-100 clean environment. All tubing and filters were acid-washed before use. Samples were acidified to pH 1.7 with high-purity HCl (Seastar) within six months of sampling and stored at room temperature for at least eight months before analysis.

Total dFe and dMn were measured using inductively coupled plasma mass spectrometry, as described previously<sup>26</sup>, and verified with seawater reference materials. Briefly, 13.0 ml aliquots of acidified sea water were weighed into acid-leached polypropylene centrifuge tubes, an <sup>57</sup>Fe spike was added for isotope dilution analysis and Fe and Mn were concentrated by Mg(OH)<sub>2</sub> precipitation through addition of concentrated ammonium hydroxide (Seastar). After repeated centrifugation and decanting, the pellet was redissolved in 5% nitric acid (Seastar) made with 1 ppb indium as a recovery standard. SAFe seawater intercalibration standards were analysed at the beginning of each analysis day with iron concentrations of 0.96 ± 0.095 nM for D2 and 0.125 ± 0.046 for S1 (n = 10), which are within the reported ranges of 0.91 ± 0.17 nM and 0.097 ± 0.043 nM (ref. 27).

The total dFe measurements from the CoFeMUG expedition were compared with earlier <sup>3</sup>He measurements along a very similar zonal section<sup>21</sup>. To separate the volcanic <sup>3</sup>He plume from background water mass variations (Supplementary Fig. S3), we used the optimum multiparameter analysis employed by ref. 21 to reconstruct the relative distributions of the water masses over the ridge (Supplementary Fig. S2). As there are questions regarding the gas solubility data<sup>28</sup> employed in component separation<sup>29</sup>, we used a more direct molar measure of excess <sup>3</sup>He by defining it as:

$${}^3\text{He}_{\text{ex}} = \delta^3\text{He} - \delta_0^3\text{He} \times 1.384 \times 10^{-8} \times C(\text{He})$$

where  $C(\text{He})$  is the concentration of helium in molar units and  $\delta^3\text{He}$  and  $\delta_0^3\text{He}$  are the helium isotope ratio anomaly and the solubility helium isotope ratio anomaly respectively, defined, for example by:

$$\delta^3\text{He} = \left( \frac{{}^3\text{He}/{}^4\text{He}_x}{{}^3\text{He}/{}^4\text{He}_A} - 1 \right) \times 100\%$$

which compares the measured helium isotope ratio to the atmospheric standard. The gridded field of volcanic <sup>3</sup>He distributions were interpolated onto the depths of our dFe and dMn samples (Fig. 2c). The estimated molar dFe:<sup>3</sup>He ratio was calculated using a type-2 linear regression for samples between the depths of 1,700 and 3,500 m and longitudes 2° W and 28° W. We explored the potential influence of the parameter weighting (including conservation of mass) in the optimum multiparameter analysis and found that varying the weights by a factor of two in both directions resulted in a change in the dFe:<sup>3</sup>He slope substantially less than the stated uncertainty of our result. The dFe:<sup>3</sup>He ratio was also calculated at closer proximity to the MAR as shown in Supplementary Table S2.

Received 31 December 2012; accepted 21 June 2013;  
published online 18 August 2013

## References

- Moore, J. K. & Braucher, O. Sedimentary and mineral dust sources of dissolved iron to the World Ocean. *Biogeosciences* **4**, 1279–1327 (2008).
- Tagliabue, A. *et al.* Hydrothermal contribution to the oceanic dissolved iron inventory. *Nature Geosci.* **3**, 252–256 (2010).
- Boyle, E. A. & Jenkins, W. J. Hydrothermal iron in the deep Western South Pacific. *Geochim. Cosmochim. Acta* **72**, A107 (2008).
- Edmond, J. M., Von Damm, K. L., McDuff, R. E. & Measures, C. I. Chemistry of hot springs on the East Pacific Rise and their effluent dispersal. *Nature* **297**, 187–191 (1982).
- German, C. R. *et al.* Heat, volume and chemical fluxes from submarine venting: A synthesis of results from the Rainbow hydrothermal field, 36° N MAR. *Deep Sea Res.* **57**, 518–527 (2010).
- Elderfield, H. & Schultz, A. Mid-ocean ridge hydrothermal fluxes and the chemical composition of the ocean. *Annu. Rev. Earth. Planet. Sci.* **24**, 191–224 (1996).
- Field, M. P. & Sherrell, R. M. Dissolved and particulate Fe in a hydrothermal plume at 9° 45' N, East Pacific Rise: Slow Fe(II) oxidation kinetics in Pacific plumes. *Geochim. Cosmochim. Acta* **64**, 619–628 (2000).
- Bennett, S. A. *et al.* The distribution and stabilisation of dissolved Fe in deep-sea hydrothermal plumes. *Earth Planet. Sci. Lett.* **270**, 157–167 (2008).
- Statham, P. J., German, C. R. & Connelly, D. P. Iron (II) distribution and oxidation kinetics in hydrothermal plumes at the Kairei and Edmond vent sites, Indian Ocean. *Earth Planet. Sci. Lett.* **236**, 588–596 (2005).
- Wu, J., Wells, M. L. & Rember, R. Dissolved iron anomaly in the deep tropical-subtropical Pacific: Evidence for long-range transport of hydrothermal iron. *Geochim. Cosmochim. Acta* **75**, 460–468 (2011).
- Klunder, M., Laan, P., Middag, R., Baar, H. J. W. D. & Ooijen, J. V. Dissolved iron in the Southern Ocean (Atlantic sector). *Deep-Sea Res. II* **58**, 2678–2694 (2011).
- Boyle, E. A., Bergquist, B. A., Kayser, R. A. & Mahowald, N. Iron, manganese, and lead at Hawaii Ocean Time-series station ALOHA: Temporal variability and an intermediate water hydrothermal plume. *Geochim. Cosmo. Acta* **69**, 933–952 (2005).
- Sander, S. G. & Koschinsky, A. Metal flux from hydrothermal vents increased by organic complexation. *Nature Geosci.* **4**, 145–150 (2011).
- Yucel, M., Gartman, A., Chan, C. S. & Luther, G. W. Hydrothermal vents as a kinetically stable source of iron-sulphide-bearing nanoparticles to the ocean. *Nature Geosci.* **4**, 367–371 (2011).
- Devey, C. W. *et al.* Diversity of Hydrothermal Systems on Slow-spreading Ocean Ridges (AGU Monograph, 2010).
- Lupton, J. Hydrothermal helium plumes in the Pacific Ocean. *J. Geophys. Res.* **103**, 15853–15868 (1998).

17. Klinkhammer, G., Rona, P., Greaves, M. & Elderfield, H. Hydrothermal manganese plumes in the Mid-Atlantic Ridge rift valley. *Nature* **314**, 727–731 (1985).
18. German, C. R. *et al.* Hydrothermal activity on the southern Mid-Atlantic Ridge: Tectonically- and volcanically-controlled venting at 4–5°S. *Earth Planet. Sci. Lett.* **273**, 332–344 (2008).
19. Melchert, B. *et al.* First evidence for high-temperature off-axis venting of deep crustal/mantle heat: The Nibelungen hydrothermal field, southern Mid-Atlantic Ridge. *Earth Planet. Sci. Lett.* **275**, 61–69 (2008).
20. Haase, K. M. *et al.* Diking, young volcanism and diffuse hydrothermal activity on the southern Mid-Atlantic Ridge: The Lilliput field at 9°33' S. *Mar. Geol.* **266**, 52–64 (2009).
21. Ruth, C., Well, R. & Roether, W. Primordial <sup>3</sup>He in South Atlantic deep waters from sources on the Mid-Atlantic Ridge. *Deep-Sea Res.* **47**, 1059–1075 (2000).
22. Lupton, J. E., Pyle, D. G., Jenkins, W. J., Greene, R. & Evans, L. Evidence for an extensive hydrothermal plume in the Tonga-Fiji region of the South Pacific. *Geochem. Geophys. Geosyst.* **5**, Q01003 (2004).
23. Kuma, K., Nishioka, J. & Matsunaga, K. Controls on iron(III) hydroxide solubility in seawater: The influence of pH and natural organic chelators. *Limnol. Oceanogr.* **41**, 396–407 (1996).
24. Keir, R. S. *et al.* Flux and dispersion of gases from the 'Drachenschlund' hydrothermal vent at 8° 18' S, 13° 30' W on the Mid-Atlantic Ridge. *Earth Planet. Sci. Lett.* **270**, 338–348 (2008).
25. Douville, E. *et al.* The rainbow vent fluids (36° 14' N, MAR): The influence of ultramafic rocks and phase separation on trace metal content in Mid-Atlantic Ridge hydrothermal fluids. *Chem. Geol.* **184**, 37–48 (2002).
26. Saito, M. A. & Schneider, D. L. Examination of precipitation chemistry and improvements in precision using the Mg(OH)<sub>2</sub> preconcentration ICP-MS method for high-throughput analysis of open-ocean Fe and Mn in seawater. *Anal. Chim. Acta* **565**, 222–233 (2006).
27. Johnson, K. S. *et al.* Developing iron standards for seawater. *EOS Trans.* **88**, 131–132 (2007).
28. Hamme, R. C. & Emerson, S. The solubility of neon, nitrogen and argon in distilled water and seawater. *Deep-Sea Res.* **51**, 1517–1528 (2004).
29. Roether, W., Well, R., Putzka, A. & Ruth, C. Component separation of oceanic helium. *J. Geophys. Res.* **103**, 27931–27946 (1998).
30. Chever, F. *et al.* Physical speciation of iron in the Atlantic sector of the Southern Ocean along a transect from the subtropical domain to the Weddell Sea Gyre. *J. Geophys. Res.* **115**, C10059 (2010).

### Acknowledgements

We are indebted to the captain and crew of the RV *Knorr* for their considerable efforts in the sampling of this zonal section. We also thank P. Lam, C. Hammerschmidt and A. Cox for assistance at sea, S. Birdwhistell for assistance in the WHOI inductively coupled plasma mass spectrometry facility and C. German, C. Devey and G. Henderson for conversations. We thank the GEOTRACES community and intercalibration programme. We thank J. Resing for comments. This research was financially supported by the US NSF-Chemical Oceanography programme (OCE-0452883, OCE-0752291, OCE-0928414, OCE-1031271 and OCE-1233261) and the Gordon and Betty Moore Foundation Grant @2724.

### Author contributions

The ocean section sampling expedition plan was designed by M.A.S. and C.H.L. The field sampling programme was orchestrated and implemented by T.J.G., M.A.S., C.H.L. and A.E.N. (also see Acknowledgements). Fe and Mn analyses were made by A.E.N. Optimum multiparameter analysis and gridding analyses were conducted by W.J.J. A.T. analysed the NEMO-PISCES model output comparison. Data analysis and interpretation was conducted by M.A.S., W.J.J., A.T., A.E.N. and C.H.L. The manuscript was written by M.A.S., W.J.J., A.T., A.E.N. and C.H.L.

### Additional information

Supplementary information is available in the [online version of the paper](#). Reprints and permissions information is available online at [www.nature.com/reprints](http://www.nature.com/reprints). Correspondence and requests for materials should be addressed to M.A.S. or W.J.J.

### Competing financial interests

The authors declare no competing financial interests.